

AIR FORCE
TECHNICAL DATA CENTER

TECHNICAL LIBRARY

Document No. 61-03-5430

Copy No. X

578 CARD

27

Technical Report No. 32-58

**Review of Results of an Early Rocket Engine
Film-Cooling Investigation at the
Jet Propulsion Laboratory**

William E. Welsh, Jr.

FACILITY FORM 502

N65-82290
(ACCESSION NUMBER)

29
(PAGES)

AD-814146
(NASA CR OR TMX OR AD NUMBER)

CB. 60939

(THRU) _____

None
(CODE)

(CATEGORY) _____

jpl

JET PROPULSION LABORATORY
CALIFORNIA INSTITUTE OF TECHNOLOGY
PASADENA, CALIFORNIA

March 13, 1961


61035-430

NATIONAL AERONAUTICS AND SPACE ADMINISTRATION
CONTRACT NO. NASW-6

Technical Report No. 32-58

**Review of Results of an Early Rocket-Engine
Film-Cooling Investigation at the
Jet Propulsion Laboratory**

William E. Welsh, Jr.


Donald R. Bartz, Chief
Liquid Propulsion Research

JET PROPULSION LABORATORY
CALIFORNIA INSTITUTE OF TECHNOLOGY
PASADENA, CALIFORNIA

March 13, 1961

Copyright © 1961
Jet Propulsion Laboratory
California Institute of Technology

CONTENTS

I. Introduction	1
II. Experimental Apparatus	1
A. Thrust Chamber	1
B. Film-Coolant Injectors	1
C. Heat-Transfer-Measurement Apparatus	2
D. Film-Coolant-Flow Apparatus	2
E. Rocket-Engine-Control Apparatus	2
III. Experimental Procedure	2
A. Engine Operation	2
B. Film-Coolant Flow-Rate Adjustment	2
C. Heat-Transfer Measurement	3
D. Outline of Experimental Tests	3
E. Experimental Errors	3
IV. Experimental Results	4
A. Local Reduction in Heat Flux	4
B. Comparison of Cooling Performance of Injector Types	4
C. Comparison of Cooling Performance of Coolant Types	4
D. Comparison of Effect of Various Film Coolants on Engine Performance	5
E. Comparison With Results of Other Investigators	5
V. Conclusions	7
Nomenclature	7
References	8

TABLES

1. Specifications for film-coolant injectors	2
2. Calculated inner-surface area of cooled motor-wall segments	3
3. List of experimental tests	3
4. Film-coolant properties: enthalpy rise from injection state to vaporized state and viscosity	5

FIGURES

1. Rocket motor with sectional cooling jacket and film-coolant injectors for quantitative heat-transfer analysis	9
2. Rocket-motor components	9
3. Nozzle-inner-wall contour	10
4. Film-coolant injector with deflector	10
5. Film-coolant injector without deflector	11
6. Designation of film-cooling stations and external cooling segments	11
7. Typical heat-flux distribution with no film coolant injected	11
8. Typical heat-flux reduction with water film-coolant injected from Injector 1 at Station 2	12
9. Local reduction in heat flux; water, Injector 1, Station 2	12
10. Local reduction in heat flux; water, Injector 2, Station 2	12
11. Local reduction in heat flux; water, Injector 3, Station 2	12
12. Local reduction in heat flux; water, Injector 4, Station 2	13
13. Local reduction in heat flux; water, Injector 5, Station 2	13
14. Local reduction in heat flux; water, Injector 6, Station 2	13
15. Local reduction in heat flux; water, Injector 7, Station 2	13
16. Local reduction in heat flux; water, Injector A, Station 1	14
17. Local reduction in heat flux; water, Injector B, Station 1	14
18. Local reduction in heat flux; water, Injectors B and 5, Stations 1 and 2	14
19. Local reduction in heat flux; water, Injectors B and 5, Stations 1 and 2	14
20. Local reduction in heat flux; aniline-alcohol, Injector 5, Station 2	15
21. Local reduction in heat flux; aniline-alcohol, Injector 6, Station 2	15
22. Local reduction in heat flux; aniline-alcohol, Injector B, Station 1	15
23. Local reduction in heat flux; 60-octane gasoline, Injector 5, Station 2	15
24. Local reduction in heat flux; 60-octane gasoline, Injector B, Station 1	16
25. Local reduction in heat flux; methyl alcohol, Injector 5, Station 2	16
26. Local reduction in heat flux; methyl alcohol, Injector B, Station 1	16
27. Local reduction in heat flux; ammonia, Injector 5, Station 2	16
28. Local reduction in heat flux; ammonia, Injector B, Station 1	17
29. Local reduction in heat flux; jet fuel, Injector 5, Station 2	17
30. Local reduction in heat flux; water, Injector 5, Station 3	17

FIGURES (Cont'd)

31. Local reduction in heat flux; water, Injector 5, Station 4	17
32. Local reduction in heat flux; water, Injectors B and 5, Stations 1 and 3	18
33. Comparison of performance of all injectors with water used as film coolant	18
34. Comparison of organic film-coolant performance	18
35. Comparison of local cooling performance of all coolant types	19
36. Cooling effectiveness K for all coolants, where $K = (Q_0 - Q_{\text{cooled}}) / \{ \dot{w}_{fc} [h_{fg} + c_p(T_{\text{sat}} - T_{\text{inj}})] \}$	19
37. Motor-performance decrease with film cooling	20
38. Film patterns on nozzle surface	20
39. Stanton number comparison with NACA results	21

FOREWORD

This Report reviews film-cooling data obtained by JPL between 1947 and 1949 by E. Lynn Wilson and Robert H. Boden. Initial results were published in JPL internal publications; later results were summarized in draft form by Wilson and Boden before their departure from JPL. The data presented in that draft have been reviewed, correlated, and interpreted by the present author in order to compare the results using different injector types and cooling, and to compare the results with existing theory and previously published correlations of data obtained in constant-area ducts.

ABSTRACT

The experimental rocket-engine film-cooling data of E. L. Wilson and R. H. Boden are reviewed in order to aid in establishing an understanding of the qualitative nature of film cooling in rocket-engine thrust chambers. The experimental engine was operated at approximately 1000-lb thrust, burning aniline-alcohol fuel and red fuming nitric acid oxidizer at 316-psia chamber pressure. The experimental data consist of measured reductions in local heat flux resulting from the introduction of liquid film coolant on the inner wall. Six film coolants were tested. These included water, aniline-alcohol fuel, 60-octane gasoline, methyl alcohol, anhydrous ammonia, and AN 58 or JP-3 jet fuel. The coolant was injected at several flow rates up to 7% of the engine propellant flow rate from a series of drilled holes around the inner wall at one or more axial locations. Local heat flux was measured using segmented cooling passages for which individual coolant-flow metering and temperature measurement allowed calorimetric calculations. A heat-flux reduction of 75% was noted at the nozzle throat using water film coolant. A comparison of reduction of total heat rate to the engine walls with the calculated nonreacting enthalpy rise of film coolants from the injection state to complete vaporization coolant effectiveness ranged from 10 to 97%, the higher values being observed in the organic coolants. Gaseous dissociation and wall-coating characteristics of the organic coolants may have contributed to the measured heat-flux reduction. The use of a deflector ring which forced the coolant to flow axially along the motor walls caused a noticeable increase in coolant effectiveness. The introduction of film coolant was found to cause a smaller decrease in specific impulse than would occur if the coolant had remained inactive chemically, thermally, and mechanically.

I. INTRODUCTION

Film cooling is one method of reducing the rate of heat transfer from rocket-engine combustion products to the thrust-chamber wall. In order to accomplish the film cooling a liquid is injected at the inner surface of the wall at one or more axial locations, forming a film between the hot gases and the wall downstream of the injection point. Graham and Zucrow (Ref. 2) have recently summarized the several analytical techniques currently available for prediction of film-coolant flow-rate requirements for constant-area duct flow. The application of these techniques to rocket-engine cooling has not thus far been verified experimentally. The results of experiments reviewed in this Report are not directly comparable with the analytical results; however, a preliminary understanding of the qualitative characteristics of film cooling is furnished.

For these experiments, a rocket engine of 1000-lb thrust was utilized which operated at 316-psia chamber pressure and burned 80% aniline-20% furfuryl alcohol fuel and red fuming nitric acid (RFNA) oxidizer. The engine-cooling jacket was segmented to allow local measurements of heat-transfer rates by calorimetry. The local

heat-transfer rate to the individual cooling passages divided by the wall-surface area cooled by that passage yielded the local heat flux. The distribution of heat flux along the engine length was measured in this manner to determine the effect of film coolant on heat transfer.

Several types of film-coolant injectors were tested, each of which injected coolant through multiple drilled holes distributed around the inner wall at one or more axial locations in the engine. In two film-coolant injectors a deflector ring was added inside the ring of drilled holes to force the coolant to flow axially along the wall. Also tested were film-coolant injectors with holes positioned at an angle of 70 deg to a radial line in the diametral plane, causing a swirling flow of the injected coolant. Six film coolants were tested. These included water, methyl alcohol, 60-octane gasoline, 80% aniline and 20% furfuryl alcohol, anhydrous ammonia, and AN-58 (JP-3) jet fuel.

The results of the experiments have been reduced to dimensionless form to emphasize the comparison between effects of different film-coolant injectors and coolants. No comprehensive correlation was achieved by rendering the results dimensionless.

II. EXPERIMENTAL APPARATUS

A. Thrust Chamber

The experimental engine was designed for a nominal thrust of 1000 lb at 316-psia chamber pressure, burning aniline-alcohol fuel and RFNA oxidizer at 2.80 mixture ratio. Additional specifications were:

Characteristic velocity c^*	4500 ft/sec
Thrust coefficient C_F	1.35 (14.0-psia exhaust)
Characteristic chamber length L^*	108 in.
Chamber diameter d_c	5 in.
Contraction ratio	8:1
Nozzle-throat diameter d_*	1.767 in.
Expansion half-angle	15 deg
Nozzle-exit diameter d_e	3.700 in.

A functional sketch and a photograph of the engine are shown in Fig. 1 and 2. These figures show the segmented cooling passages in the chamber and nozzle. Each passage cooled a discrete axial increment of the inner wall. The chamber passages were sealed by compressing rubber O-rings radially on the sides of each passage with a bolted outer casing. The propellant injector was an 8-pair impinging-stream unit with no splash plate. The constant-diameter-chamber portion was comprised of four separate rings of 3-in. length bolted together. The nozzle had a continuous inner surface, as shown in Fig. 3.

B. Film-Coolant Injectors

The liquid film coolant was introduced by means of several types of injectors. One group of film-coolant injec-

tors was built for installation in the constant-diameter chamber; these are designated as chamber injectors. In the nozzle, injection holes were drilled through the wall at a location midway between the nozzle entrance and throat. This injector was therefore an integral part of the nozzle, as shown in Fig. 3, and is designated as a nozzle injector. Several of the chamber injectors included an inner ring, termed a deflector plate, designed to force the coolant to flow axially before entering the engine. Chamber injectors with and without deflector plates are shown in Fig. 4 and 5, respectively. The specific design features of each injector are listed in Table 1. Chamber injectors are numbered 1 through 6, and nozzle injectors are lettered A and B. Chamber injectors numbered 2 and 4 used holes drilled at an angle of 70 deg off the radial direction in the diametral plane to impart a circumferential or swirling component to the motion of the injected liquid. Flow-visualization tests showed that all coolant injectors produced satisfactorily symmetrical injection patterns.

Table 1. Specifications for film-coolant injectors

Injector No.	No. of holes	Hole orientation	Hole diameter, in.	Deflector installed
1	16	Radial	0.0635	No
2	16	70 deg off radial	0.0635	No
3	16	Radial	0.0635	Yes
4	16	70 deg off radial	0.0635	Yes
5	32	Radial	0.0465	No
6	48	Radial	0.0320	No
7	48	Radial	0.0380	No
A	16	Radial	0.0635	No
B	32	Radial	0.0465	No

C. Heat-Transfer-Measurement Apparatus

Calorimetry was used to determine the rate of heat transfer to each cooling passage. Coolant flow rate was measured by rotameters, and coolant-temperature rise was indicated by thermocouples immersed in the inlet and outlet streams. The heat-transfer rate was divided by the inner-wall area corresponding to that cooling passage to obtain the local heat flux. For some tests a possible source of error existed in the flow-rate value used for this calculation, since a small transfer of coolant may have occurred between coolant passages in the nozzle. The experimenters performed dye tests for such leakage and eliminated it by application of liquid sealing material.

D. Film-Coolant-Flow Apparatus

The specified film coolant was piped from gas-pressurized storage tanks to the film-coolant injector in the engine. This flow was controlled by a manually operated valve and metered by a rotameter.

E. Rocket-Engine-Control Apparatus

Chamber pressure and mixture ratio were controlled closely in order that the engine operate at constant conditions for the duration of these tests. These parameters were held within 1% of specified average values by manual control. Metering orifices and electronic pressure transducers were used to measure propellant flows. The aniline-alcohol fuel was pumped by a centrifugal pump from a storage tank, while the RFNA oxidizer was fed from a gas-pressurized tank. Thrust was measured hydraulically by means of a piston and cylinder attached to the engine mounting.

III. EXPERIMENTAL PROCEDURE

A. Engine Operation

Typical test durations were 200 sec. After an initial 20-sec period for establishment of steady-state conditions, six successive film-coolant flow rates were set. Each film-coolant flow-rate setting occupied a 30-sec period. Chamber pressure and mixture ratio were adjusted to nominal values of 316 and 2.82 psia, respectively.

B. Film-Coolant Flow-Rate Adjustment

A problem was encountered in starting the engine without concurrent starting of film-coolant flow. When

the film coolant was a fuel, starting of the engine after initiating the coolant flow resulted in a "hard start" due to excess fuel in the chamber. Conversely, with any film coolant, starting the engine before the coolant flow resulted in plugging of the injection holes with carbonaceous combustion products. A negligible flow of film coolant was started coincident with the engine in order to overcome these difficulties. After the initial 20-sec period the film-coolant flow was adjusted to its maximum setting, allowed to remain constant for 30 sec, and then changed to the next lower flow rate. A similar procedure was followed for the four succeeding flow rates.

C. Heat-Transfer Measurement

The rate of heat transfer to each externally cooled segment of the engine was measured during the initial 20-sec period and during each 30-sec coolant-flow period to determine the effect of film-coolant flow on heat flux. The wall-surface area of each cooled segment was calculated in order to determine local heat flux and is shown in Table 2. The cooled segments are designated by Roman numerals I through XII, with I representing the upstream combustion-chamber segment and XII the segment of the nozzle adjacent to the nozzle exit.

Table 2. Calculated inner-surface area of cooled motor-wall segments

Segment	Area, in. ²
I-IV	47.2 each
V	17.93
VI	11.73
VII	8.36
VIII	5.38
IX	5.67
X	7.05
XI	8.45
XII	11.46

D. Outline of Experimental Tests

Each test of 200-sec duration yielded information on the reduction of heat flux caused by the introduction of film coolant from one or more injectors for six different flow rates of a given film coolant. Twenty-four tests are reported. Table 3 indicates the film-cooling conditions in all tests. Figure 6 shows the location and designation of film-cooling injectors and external cooling segments.

E. Experimental Errors

It was felt by the experimenters that the particular propellant injector used in these tests caused non-uniform flow of the combustion products in the chamber. This could have had a detrimental effect on films injected into the combustion chamber, but it was considered that any non-uniformity would be damped out to a great extent at the nozzle inlet.

A thin layer of carbonaceous solid material (about 0.010 in. thick) was found on the engine wall after each test. It is apparent that this layer reached an equilibrium thickness during the initial 20-sec period of each test, since the heat-transfer rates measured at the end of that period without film cooling were steady and reproducible. A

carbonaceous layer reduces the rate of heat transfer without film cooling. If the film coolant flowing over such a layer does not affect the layer significantly, the further reduction of heat flux may be ascribed to the film itself; the analysis of these test results included this assumption.

In preliminary tests a wall-deposition problem was caused by $\text{Fe}(\text{NO}_3)_3$ contaminants in the RFNA. This was eliminated by using aluminum storage tanks rather than tanks constructed of ferrous materials.

The errors in measurements of pressures, flow rates, temperatures, and thrust are estimated to have been of the order of 1%. It was found that the normal test variations in chamber pressure and mixture ratio had a negligible effect on heat-flux measurements.

Table 3. List of experimental tests

Test No.	Injector No.	Injection station	Film coolant	Heat flux reported for segment	Comments
1	1	2	Water	V-X	Equal flows to each coolant injector Injector flows proportional to circumference Injector flows proportional to circumference
2	2	2	"	V-X	
3	3	2	"	V-X	
4	4	2	"	V-X	
5	5	2	"	V-X	
6	5	3	"	IV-X	
7	5	4	"	III-X	
8	6	2	"	V-X	
9	7	2	"	V-X	
10	A	1	"	VII-X	
11	B	1	"	VII-X	
12	B, 5	1, 2	"	V-X	
13	B, 5	1, 2	"	V-X	Equal flows to each coolant injector Injector flows proportional to circumference Injector flows proportional to circumference
14	B, 5	1, 3	"	IV-X	
15	5	2	Aniline-alcohol	V-X	
16	6	2	"	V-X	
17	B	1	"	VII-X	
18	5	2	60-octane gasoline	V-X	
19	B	1	"	VII-X	
20	5	2	Methyl alcohol	V-X	
21	B	1	"	VII-X	
22	5	2	Anhydrous ammonia	V-X	
23	B	1	"	VII-X	
24	5	2	AN-58 jet fuel	V-X	

IV. EXPERIMENTAL RESULTS

The experimental results report the local reductions in heat flux due to film cooling, the reduction in total heat-transfer rate to the engine, and the decrease of engine performance due to the introduction of film coolant.

A. Local Reduction in Heat Flux

A representative distribution of local heat flux along the engine length without film cooling is shown in Fig. 7 as taken from the data of Test No. 1. Heat flux without film cooling was within 6% of this distribution in all tests. A curve representing an analytical prediction of heat flux based on the method of Ref. 3 is also shown in Fig. 7. Most of the discrepancy between the data and the prediction is ascribed to the insulating carbon deposition. The abscissa is designated as fractional surface area, with a value of zero at the upstream end of the chamber and a value of unity at the nozzle exit. A typical plot of reduction in heat flux to the nozzle only is shown in Fig. 8 for a single coolant flow-rate setting during Test No. 1. The ordinate is the fractional reduction based on the reference value of heat flux with no film cooling, q_0 , and the fractional area refers to the nozzle-surface area only. The data of Fig. 8 represent reductions in average heat flux over finite increments of surface area. A data point is shown positioned at the midpoint of each area increment. A curve has been faired through the data points to suggest the trend of cooling performance throughout the nozzle. The faired curve may be taken as representing the approximate heat flux reduction over any infinitesimal area increment, being faired through a series of averages for finite area increments.

The reduction in heat flux to the wall in all runs where coolant was injected at Stations 1 and 2 is indicated in Fig. 9 through 29. These figures use the same coordinates as Fig. 8, with simplified nomenclature.

The maximum heat-flux reduction observed in any of the tests was 75%. It occurred at the nozzle throat when water was injected from holes immediately upstream of the throat, as shown in Fig. 17. At the higher film-coolant flow rates the heat flux reduction was generally uniform for a short distance downstream of injection, then began a linear reduction with the downstream area, and vanished a short distance downstream of the nozzle throat. As an example, Fig. 11 shows this trend of performance. In some cases, again for the higher coolant flows, the heat-flux reduction increased as the nozzle throat was approached. The organic film-coolant performance, such

as shown for mixed fuel (aniline and furfuryl alcohol) in Fig. 20, was irregular in the flow direction rather than steadily decreasing as was the case with water coolant. This may have been due to a change in the initial carbonaceous wall coating due to effects of the organic coolants.

Heat-flux reductions are shown in Fig. 30, 31, and 32 for the three tests in which film coolant was injected upstream of the nozzle entrance. In these tests, the heat flux to the combustion-chamber segments, in addition to that of the nozzle, was affected by the film coolant. Here the fractional area coordinate commences at the upstream coolant injector.

B. Comparison of Cooling Performance of Injector Types

Figure 33 shows the reduction of total heat-transfer rate to the wall area downstream of the injection point vs film-coolant flow rate for water coolant injected. The flow rate is expressed as a fraction of total flow rate, where total flow is the summation of film-coolant and propellant flows. Figure 34 gives this information for the tests in which organic coolants were injected. Figure 33 shows that at a given coolant-flow rate injection from two stations downstream of the combustion chamber was the most efficient method for reducing the rate of heat transfer. Conversely, injection from a single location in the combustion chamber was the least efficient method. All tests indicated a change in slope of the cooling performance at some flow rate generally between 2 and 3% of the total flow rate. Kinney, Abramson, and Sloop (Ref. 4) observed such a discontinuity in hot-gas film-cooling tests and hypothesized a film instability at higher flow rates as a contributing factor. It is noted in Fig. 33 that injection of coolant in a swirling pattern had a negligible effect on cooling performance, although the addition of a deflector plate increased the effectiveness of the coolant.

C. Comparison of Cooling Performance of Coolant Types

The heat-flux reduction caused by coolant flowing from injector No. 5 at Station 2 is shown in Fig. 35 for all coolants tested at approximately equal flow rates. Here it is noted that the performance of the various coolants throughout the nozzle was not radically different. Water furnished the greatest reduction in throat heat flux and the reduction did not change irregularly with distance as was the case with the organic coolants. Table 4 lists

Table 4. Film-coolant properties: enthalpy rise from injection state to vaporized state and viscosity

Property	Coolant					
	Water (5, 6)*	80 % aniline 20 % furfuryl alcohol (7)	60-octane gasoline (7)	Anhydrous ammonia (7)	AN-58 jet fuel (JP-3) (7)	Methyl alcohol (8)
Injection temperature, T_{inj} , °F	70	70	70	70	70	70
Saturation temperature at 316 psia T_{sat} , °F	426	660	500	127	500	333
Liquid specific heat at $(T_{inj} + T_{sat})/2$, c_p Btu/lb °F	1	0.540	0.61	1.151	0.59	0.566
Latent heat of vapor- ization at 316 psia, h_{fg} , Btu/lb	800	138	42	442	67	487
$h_{fg} + [c_p(T_{sat} - T_{inj})]$ Btu/lb	1156	456.5	304.0	507.6	321.0	750
Viscosity at 100°F, μ , lb/ft sec	0.450×10^{-3}	1.88×10^{-3} (pure aniline)	0.329×10^{-3}	0.087×10^{-3}	0.383×10^{-3}	0.306×10^{-3}

*Numbers in parentheses refer to reference numbers of source materials.

the calculated enthalpy rise of the six coolants from injection to vaporized states, assuming no chemical changes. In view of the large differences in this enthalpy rise, or cooling potential, it is interesting to note that the levels of heat-flux reduction in Fig. 35 are not markedly different. This comparison is drawn once more in Fig. 36, where the reduction of the total heat-transfer rate is presented as a fraction of the cooling potential for each coolant. Here it is noted that the organic film coolants realized a greater portion of their cooling potential than did water. A comparison of viscosities, shown in Table 4 and Fig. 36, indicates no correlation with this cooling performance. Endothermic dissociation and additional carbon formation with the use of organic coolants offer several possible explanations of the curves of Fig. 36, although the quantitative nature of these effects cannot be estimated accurately.

D. Comparison of Effect of Various Film Coolants on Engine Performance

It is desirable that the utilization of film cooling cause a minimum reduction in the specific impulse of the engine. Figure 37 indicates the specific-impulse reduction measured in these experiments for the six film coolants. The predicted decrease of impulse, where specific impulse is based on total flow rate of propellants and coolant, for the case where the coolant undergoes no changes is also shown in this figure. Except for several points at low coolant flows, it is observed that all film coolants caused less impulse reduction than would an inert coolant. These differences are probably caused by vaporization, accel-

eration, and chemical changes undergone by the coolant as it interacts with the main stream.

E. Comparison With Results of Other Investigators

Kinney, Abramson, and Sloop (Ref. 4) have summarized the results of film-cooling experiments conducted at the National Advisory Committee on Aeronautics (NACA). Their experiments determined the amount of protection an injected film would provide against a hot gas flowing in a straight tube, in terms of the tube length covered by the film. Graham and Zucrow (Ref. 2) have shown that these NACA results may be presented in dimensionless form as:

$$St = 0.00275, \text{ smooth-surfaced tubes, } Pr_b = 1.0$$

$$St = 0.00325, \text{ rough-surfaced tubes, } Pr_b = 1.0$$

These correlations of experimental data utilize a Nusselt number based on tube diameter, main-stream thermal conductivity, and a heat-transfer coefficient deduced from the enthalpy rise of the injected coolant, protected wall area, and the temperature difference between coolant saturation and main-stream conditions. The Reynolds number for the correlation is based on main-stream conditions. Therefore, the Stanton number is

$$St = \frac{Nu}{Re Pr} = \frac{\frac{bD}{k_b}}{\frac{(\dot{w}/A)_b D}{\mu_b} Pr_b} = \frac{\frac{\dot{w}_{fc} [b_{fg} + c_p(T_{sat} - T_{inj})] D}{A_s (T_b - T_{sat}) k_b}}{\frac{(\dot{w}/A)_b D}{\mu_b} Pr_b}$$

or

$$St = \left\{ \frac{\dot{w}_{fc} [b_{fg} + c_p(T_{sat} - T_{inj})]}{(\dot{w}/A)_b (T_b - T_{sat}) (A_s)} \right\} \left(\frac{\mu}{k} \right)_b \left(\frac{1}{Pr_b} \right)$$

The surface area covered by the film was taken as the product $\pi D L$, where L is the distance in the direction of flow from the injection point. The distance L was determined by measurements of tube-wall temperature; the tube was not externally cooled; therefore, the temperature rose suddenly where the liquid film terminated. In the region covered by the liquid film the wall temperature did not exceed the water-coolant saturation temperature. Thermocouples were arranged along the tube length and circumference. Where the film was effective, it was found that the wall temperatures were uniform in both circumferential and axial directions. Two types of coolant injectors were investigated: a ring of holes with an inner deflector plate, and a porous ring. These radically different injection methods were found to yield identically cooling characteristics for equal coolant-flow rates.

In the case of a film-cooled wall which is also externally cooled it would be anticipated that where the film is effective the heat flux to the external cooling jacket would be essentially zero. This did not occur in the experiments of Boden and Wilson reviewed in this Report. The heat-flux reduction was 75% at the upper extreme of the measurements and much less for the bulk of the tests, even at locations immediately downstream of coolant injection. In order to compare these results with those of Kinney, et al (Ref. 4), it is necessary to develop a rationalization of this incomplete reduction of heat flux. Figure 38 shows the flow patterns on the wall of the exhaust nozzle, where film coolant was injected in the nozzle contraction; a circumferentially non-uniform pattern is observed in these photographs. This non-uniformity suggests that the portions of wall surface between the coolant streams were subjected to the hot-gas flow, causing some heat transfer directly to the externally cooled wall. Proceeding on the hypothesis that the fractional reduction in heat flux to a particular cooling segment is equal to the fraction of the wall area covered by the liquid film, a calculation of the Stanton number was made for those tests in which water coolant was injected. The evaporated coolant was assumed to be ineffective downstream of liquid film termination. Reynolds numbers and Nusselt numbers were calculated for the three lower coolant-flow rates of each test, thus limiting the comparison to the coolant-flow range of greater effectiveness, corresponding to the range for which the NACA correlations apply. Since the coolant film encountered variable mainstream conditions in the exhaust nozzle, it was necessary to determine average Reynolds and Nusselt numbers. This was done by weighting the average on the basis of local conditions where the fractional heat-flux

reduction was greater. The true values of local Nusselt numbers for each cooling segment could not be determined since the local rate of coolant evaporation was impossible to measure.

The results of these calculations are shown in Fig. 39, with the NACA correlations indicated for comparison. A Prandtl number of unity is used for the Stanton number in Fig. 39. It is noted that the bulk of the experimental data of Boden and Wilson lies in the region of $St = 5.5 \times 10^{-3}$ at $Re = 5.5 \times 10^5$, whereas the NACA data are near $St = 3.0 \times 10^{-3}$ at all Reynolds numbers. Therefore, the Boden and Wilson data demonstrate heat-transfer coefficients approximately 100% greater than those found by the NACA. Several explanations of this disparity are possible. First, the hypothesis for the incomplete reduction of heat flux may be erroneous; there may be a finite rate of heat transfer through the liquid film by radiation. (Very little could be transferred by convection where the wall temperatures were close to the coolant-injection and saturation temperatures.) Estimates of radiant heat transfer in rocket engines indicate that this is unlikely to be significant in the case of this engine, however. Second, if the increase in the gas-to-film heat-transfer coefficient is real, it may be the result of increased main-stream turbulence in the rocket engine or increased film turbulence and break-away due to circumferential non-uniformities in the film pattern.

Theoretical treatments of the film-cooling problem have been made by Knuth (Ref. 9), Rannie, Crocco, Schurman, Sellers (discussed in Ref. 2), and others. Graham and Zucrow (Ref. 2) have reviewed these solutions and found them, in general, somewhat complex for practical engineering applications. They then developed methods of simplifying these solutions by introducing assumptions and approximations for the case of anticipated application in rocket-motor film cooling. For a Reynolds number of 5×10^5 , they showed that the analyses of Rannie, Sellers, and Crocco indicate a Stanton number of the order of 2×10^{-3} , with a tendency of decreasing Stanton number with increasing Reynolds number. The experimental data of Boden and Wilson indicate Stanton numbers of the same order of magnitude, although several times greater than these analytical results.

Knuth (Ref. 9) performed film-coolant injection experiments to determine the critical injection velocity, which was defined as the velocity above which coolant injected from radial holes into a duct containing flowing gas penetrates into the gas stream without conforming to the downstream duct contour. A calculation has been

made using Knuth's correlation to determine whether this critical velocity was exceeded in Boden and Wilson's tests, using radial-hole injectors without deflector plates.

It was found that the critical velocity was exceeded only with coolant injector No. 6, and there only at the highest specified coolant-flow rate.

V. CONCLUSIONS

The results of these experiments are indicative of the qualitative behavior of film coolants injected from holes distributed peripherally at one or more axial locations in a rocket engine. It has been shown that coolant injection downstream of the combustion chamber provided greater local and total reductions in heat-transfer rate to the engine than did injection in the combustion chamber. A deflector ring, which causes radially injected coolant to flow in an axial path before cooling, has been shown to improve the cooling effectiveness.

The reduction in total heat-transfer rate, expressed as a fraction of enthalpy rise from injection through vaporization, was less for water than for organic coolants.

Viscosity of the coolants did not correlate this difference, but organic coolant dissociation and wall deposition conceivably contributed to the discrepancy. All coolants provided approximately equal absolute reductions in local and total heat transfer rates, with water being superior by a small margin. A comparison of deduced gas-to-film heat-transfer coefficients with water film coolant showed Stanton numbers approximately twice as great as those measured by the NACA (Ref. 4) in hot-gas straight-tube experiments.

All coolants caused less decrease of specific impulse than would be expected from injection of a substance which undergoes no chemical reaction in the engine.

NOMENCLATURE

A	area, ft ²
c_p	constant-pressure specific heat, Btu/lb _m °F
D	diameter, ft
h_{fg}	latent heat of vaporization, Btu/lb _m
h	heat-transfer coefficient, Btu/ft ² hr °F
I_{sp}	specific impulse, lb _f sec/lb _m
k	thermal conductivity, Btu/ft hr °F

q	local heat flux, Btu/in. ² sec
Q	total heat-transfer rate, Btu/sec
T	temperature, °F
V	velocity, ft/sec
\dot{w}	mass-flow rate, lb _m /sec
μ	kinematic viscosity, lb _m /ft sec
ρ	density, lb _m /ft ³

Subscripts

b	average gas-flow condition
fc	film-cooling condition
inj	injection condition
L	nozzle-exit condition
sat	saturation condition
x	local condition
0	without film-cooling
s	surface

Dimensionless Groups

A_x/A_L	fractional surface area
K	cooling effectiveness, $(Q_0 - Q_{fc})/(\dot{w}_{fc}[h_{fg} + c_p(T_{sat} - T_{inj})])$
Nu	Nusselt number, hD/k
Pr	Prandtl number, $\mu c_p/k$
$\Delta q/q_0$	fractional reduction in local heat flux
Re	Reynolds number, $\rho VD/\mu$
St	Stanton number, $Nu/(Re Pr)$

REFERENCES

1. Boden, R. H., "Heat Transfer in Rocket Motors and Application of Film and Sweat Cooling," ASME Transactions, Vol. 73, No. 4 (May 1951), pp. 385-390.
2. Graham, A. R., and Zucrow, M. J., Film Cooling, Its Theory and Application, Technical Memorandum No. 57-3, Lafayette, Indiana, Purdue University Rocket Laboratory, October 1957.
3. Bartz, D. R., "A Simplified Method of Rapid Estimation of Heat Transfer Coefficients in Rocket Nozzles," Jet Propulsion, January 1957.
4. Kinney, G. R., Abramson, A. E., and Sloop, J. L., Internal-Liquid Film-Cooling Experiments With Air-Stream Temperatures to 2000°F in 2- and 4-Inch Diameter Horizontal Tubes, NACA Report 1087, 1952.
5. Keenan, J. H., and Keyes, F. G., Thermodynamic Properties of Steam, 1st ed., N.Y., N.Y., John Wiley and Sons, 1955.
6. Eckert, E. R. G., Introduction to the Transfer of Heat and Mass, N.Y., N.Y., McGraw-Hill Book Co., Inc., 1950.
7. Liquid Propellants Handbook, Columbus, Ohio, Battelle Memorial Institute, 1955. (Confidential.) (Unclassified portions only.)
8. Hodgman, C. D. (Editor), Handbook of Chemistry and Physics, 32nd ed., Cleveland, Ohio, Chemical Rubber Publishing Company, 1950.
9. Knuth, E. L., The Mechanics of Film Cooling, Memorandum No. 20-85, Pasadena, Calif., Jet Propulsion Laboratory, 21 September 1953.

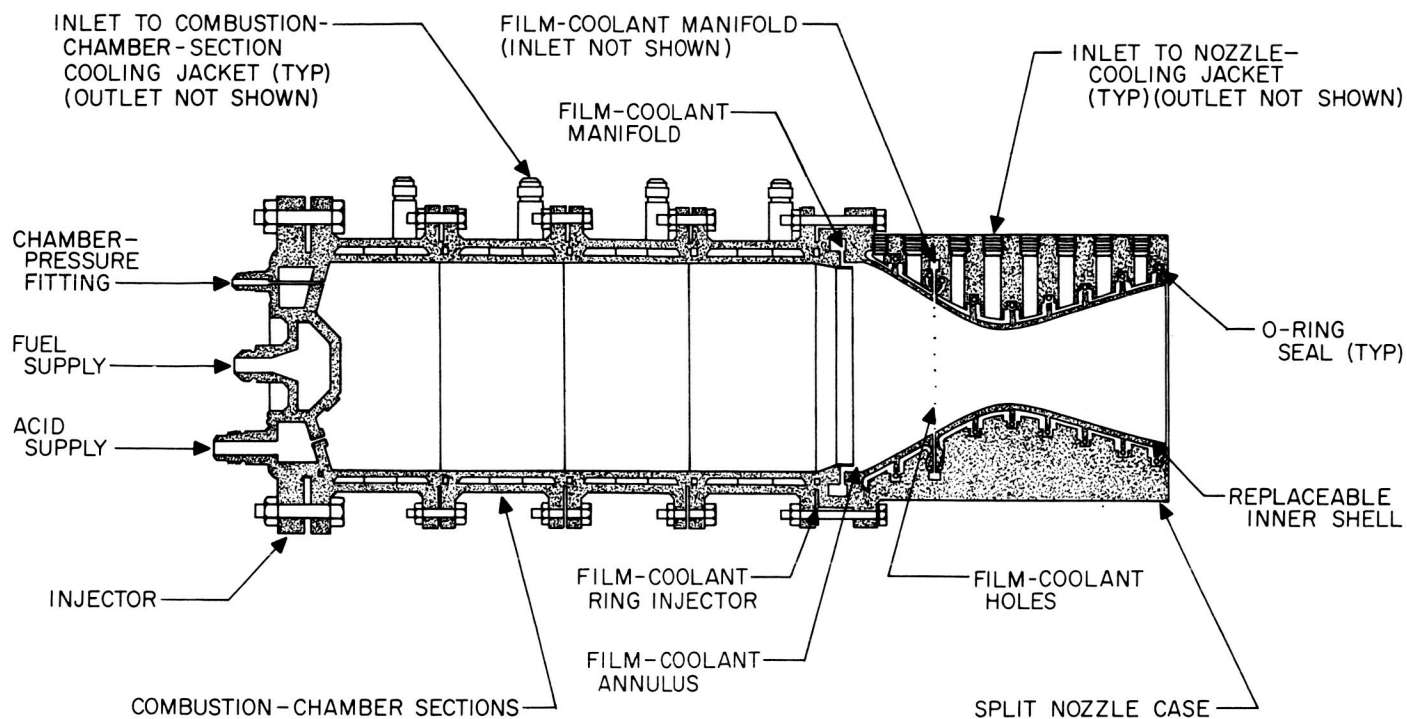


Figure 1. Rocket motor with sectional cooling jacket and film-coolant injectors for quantitative heat-transfer analysis

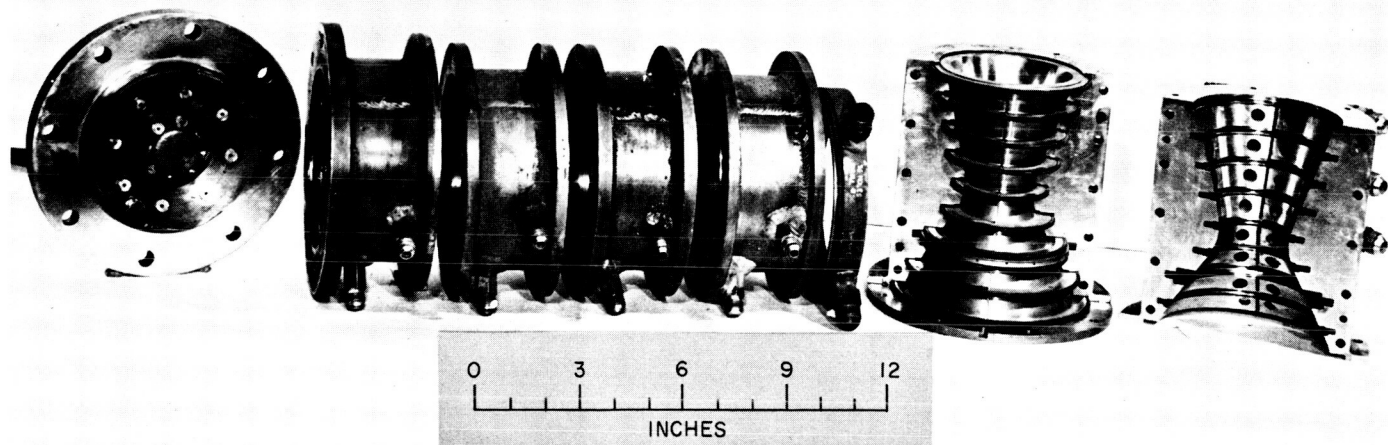


Figure 2. Rocket-motor components

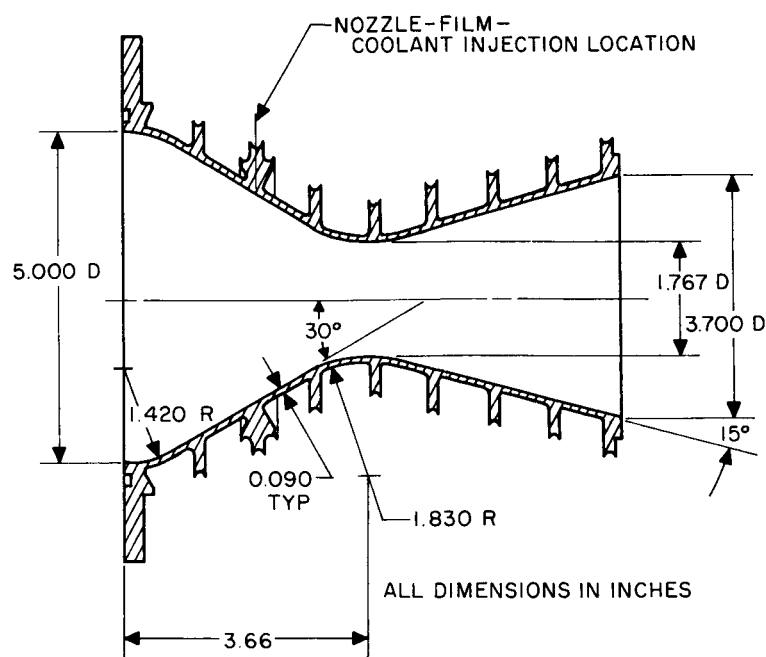


Figure 3. Nozzle-inner-wall contour

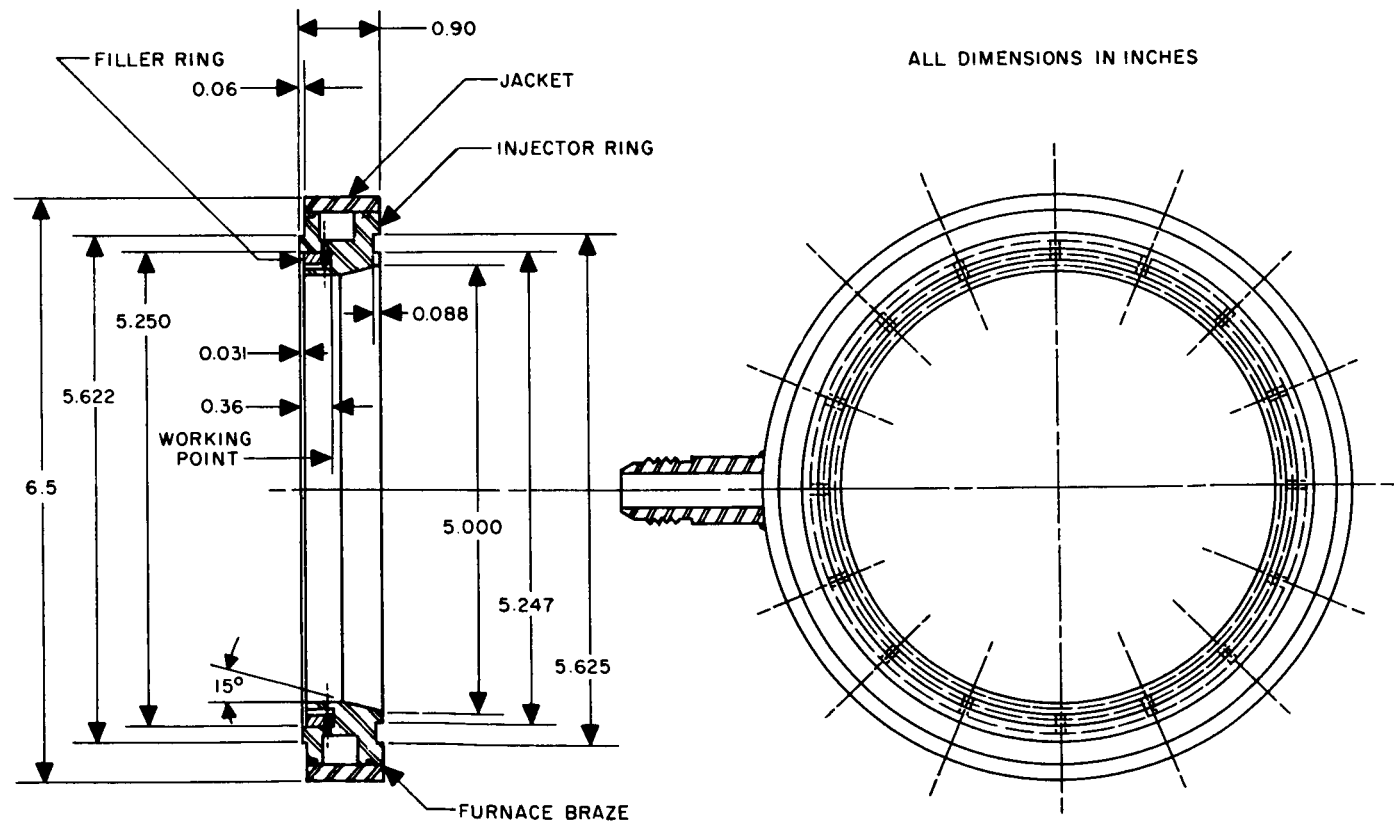


Figure 4. Film-coolant injector with deflector

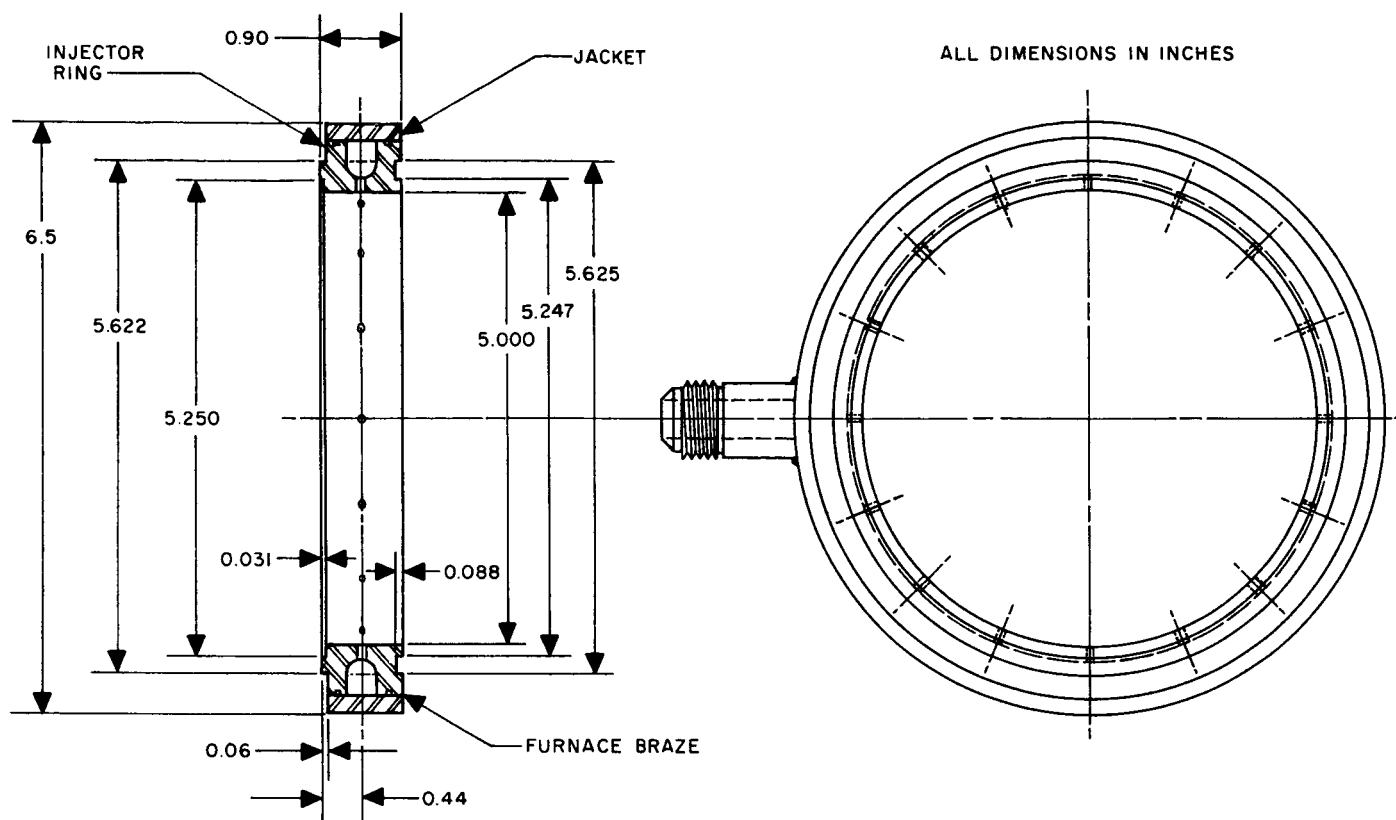


Figure 5. Film-coolant injector without deflector

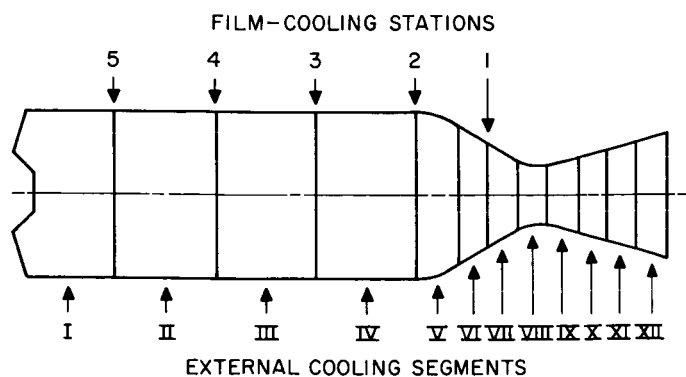


Figure 6. Designation of film-cooling stations and external cooling segments

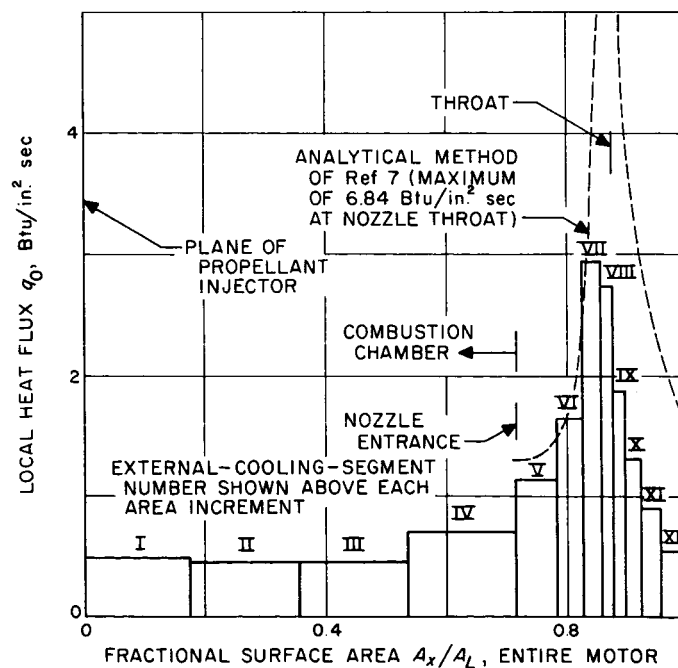


Figure 7. Typical heat-flux distribution with no film coolant injected

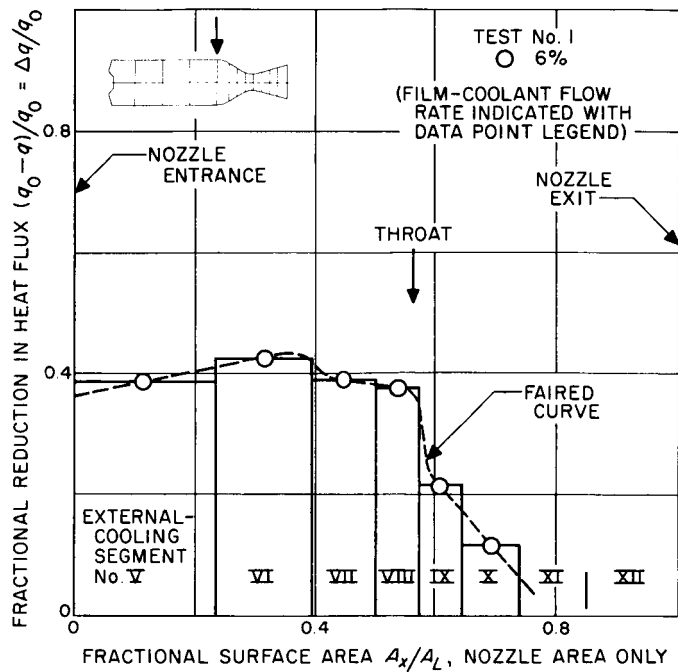


Figure 8. Typical heat-flux reduction with water film-coolant injected from Injector 1 at Station 2

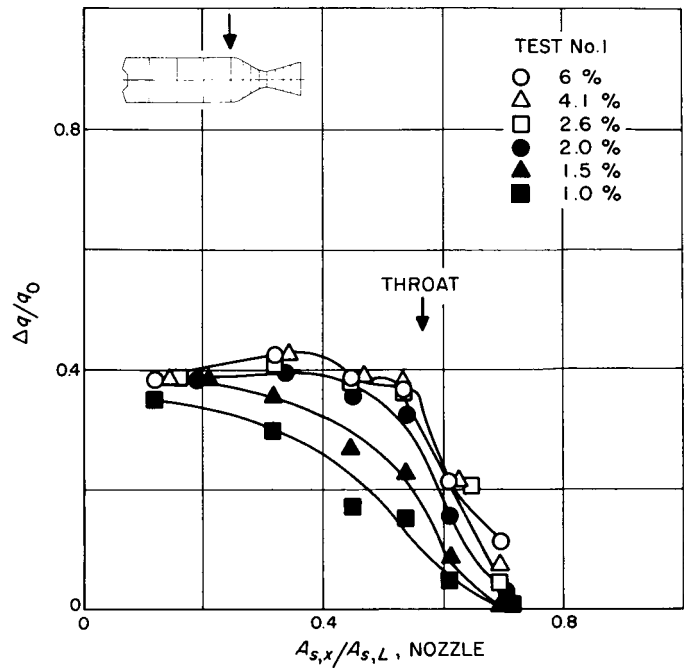


Figure 9. Local reduction in heat flux; water, Injector 1, Station 2

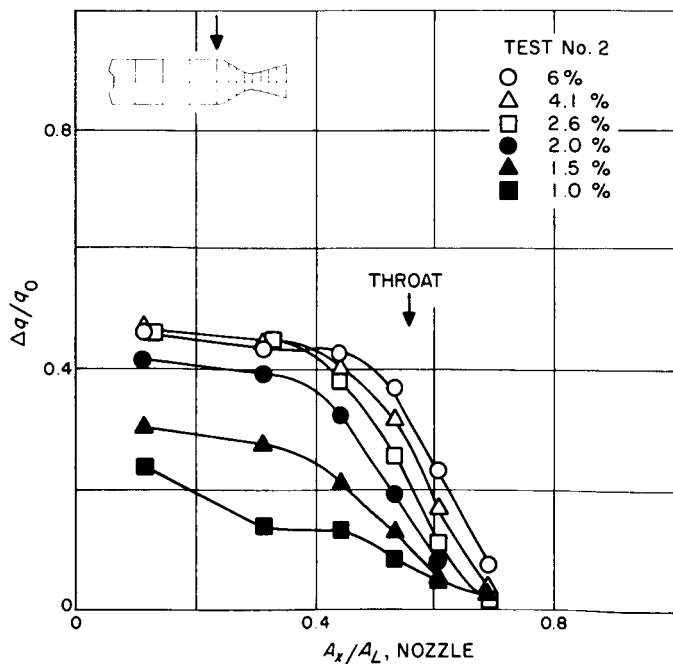


Figure 10. Local reduction in heat flux; water, Injector 2, Station 2

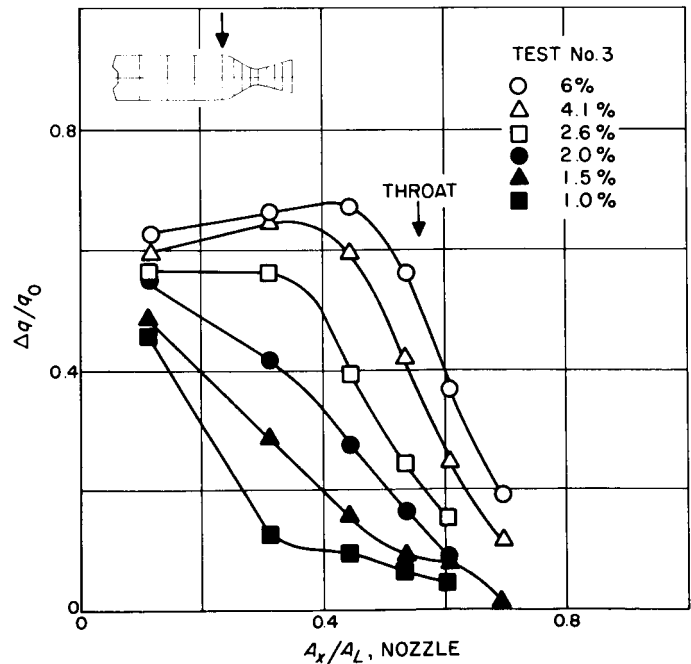


Figure 11. Local reduction in heat flux; water, Injector 3, Station 2

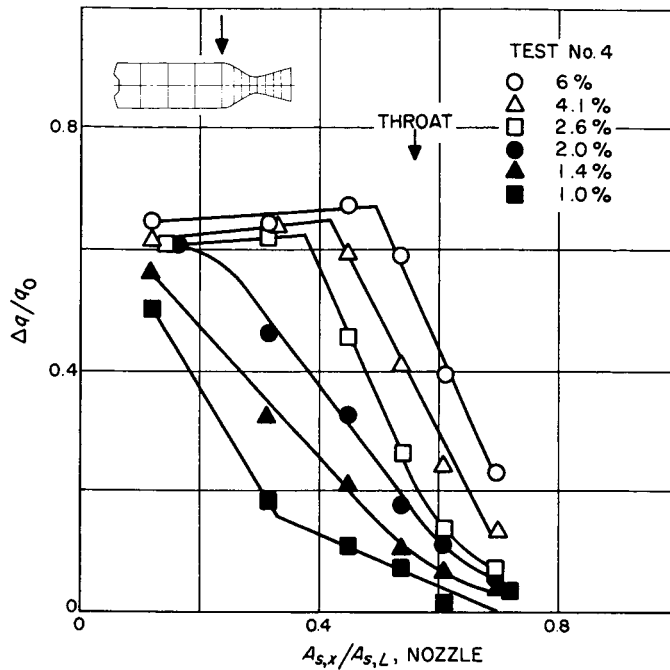


Figure 12. Local reduction in heat flux; water, Injector 4, Station 2

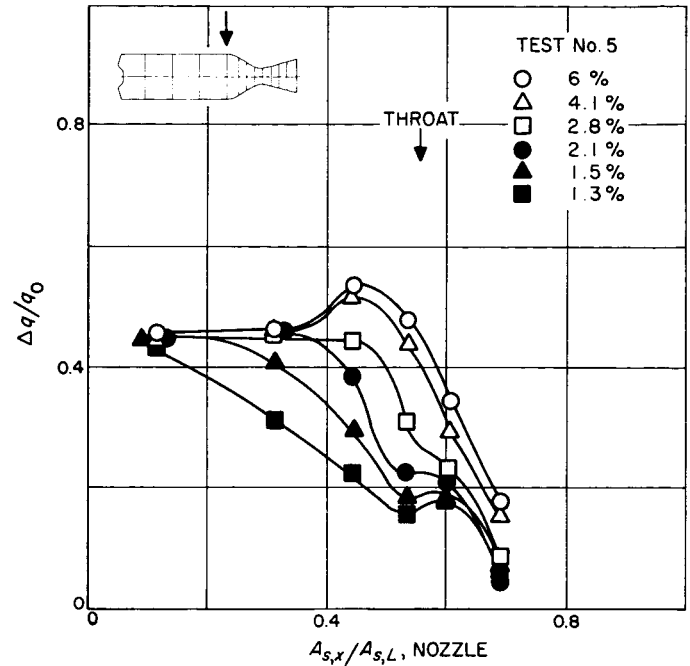


Figure 13. Local reduction in heat flux; water, Injector 5, Station 2

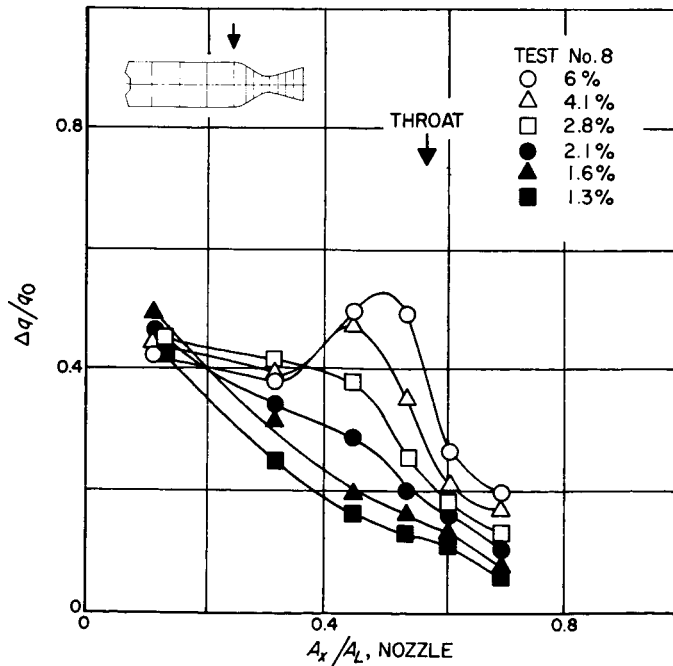


Figure 14. Local reduction in heat flux; water, Injector 6, Station 2

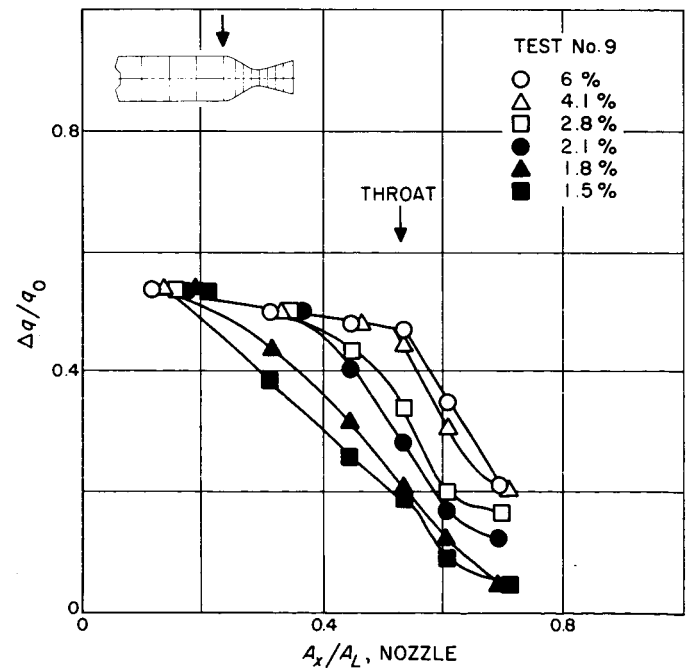


Figure 15. Local reduction in heat flux; water, Injector 7, Station 2

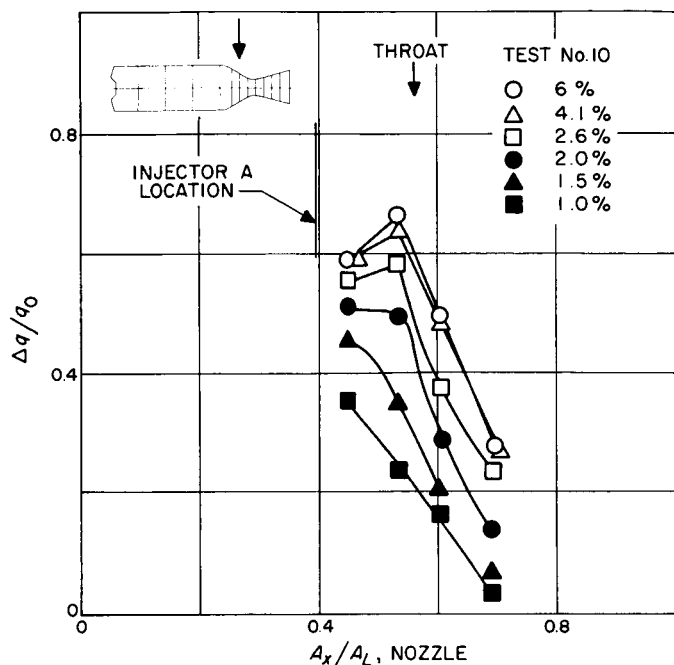


Figure 16. Local reduction in heat flux; water, Injector A, Station 1

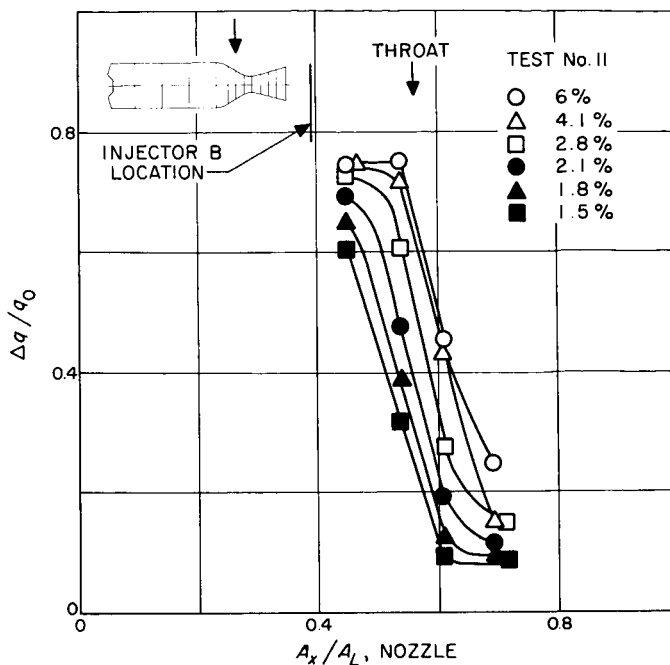


Figure 17. Local reduction in heat flux; water, Injector B, Station 1

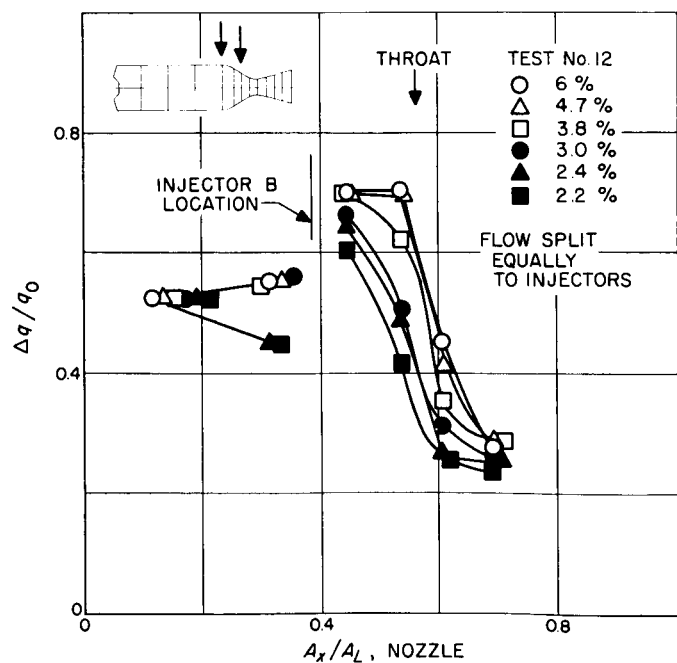


Figure 18. Local reduction in heat flux; water, Injectors B and 5, Stations 1 and 2

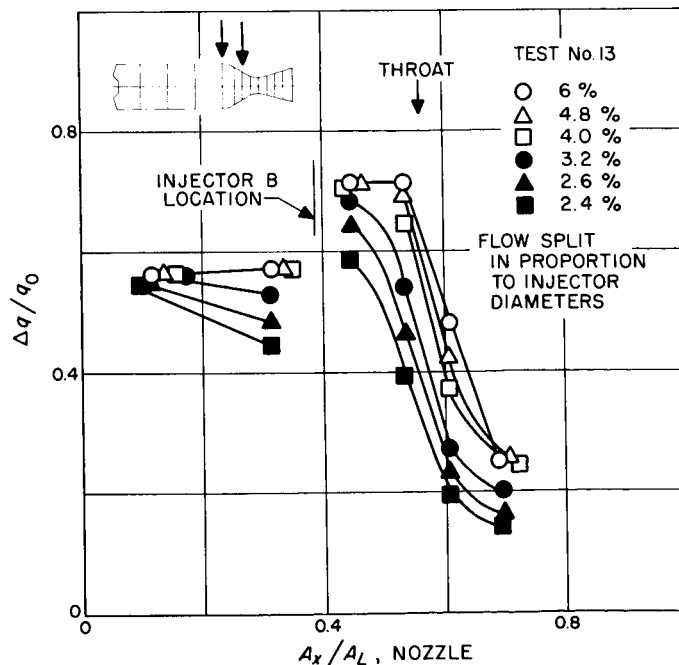


Figure 19. Local reduction in heat flux; water, Injectors B and 5, Stations 1 and 2

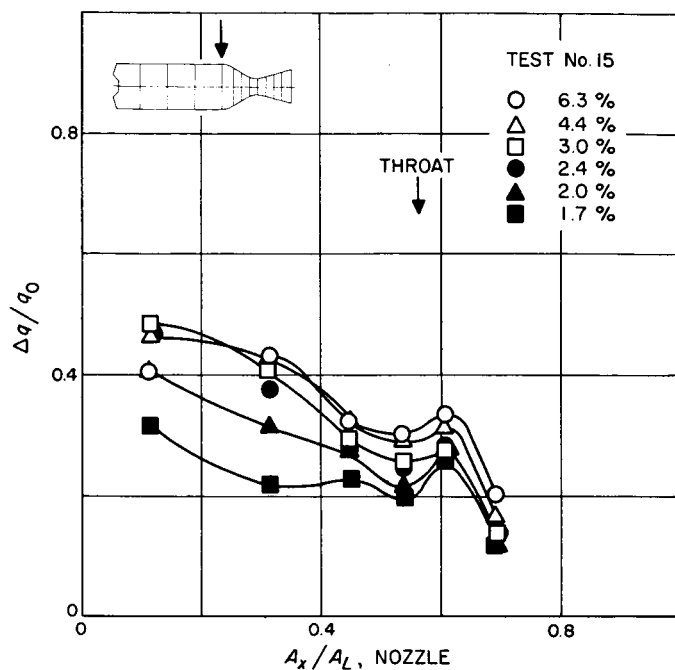


Figure 20. Local reduction in heat flux; aniline-alcohol, Injector 5, Station 2

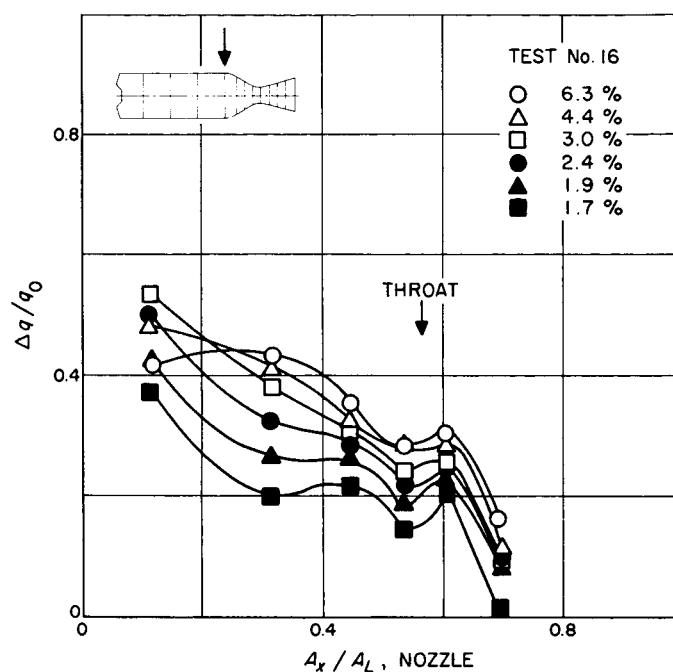


Figure 21. Local reduction in heat flux; aniline-alcohol, Injector 6, Station 2

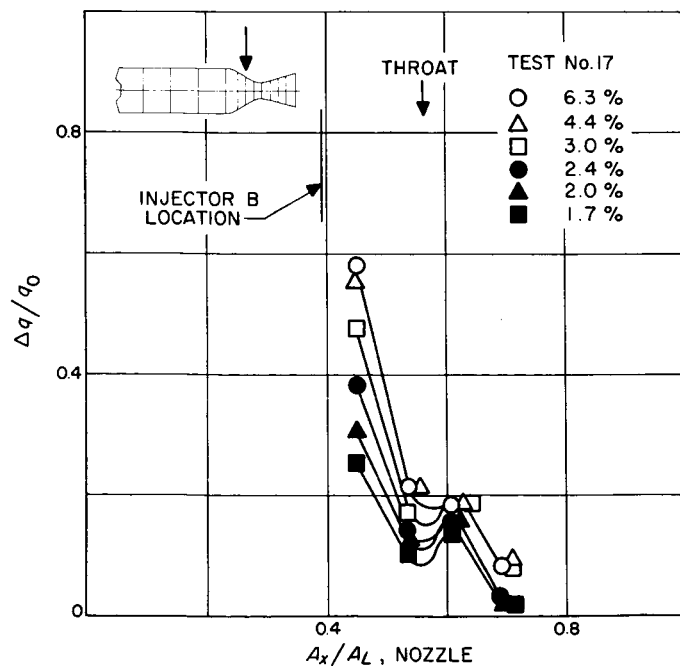


Figure 22. Local reduction in heat flux; aniline-alcohol, Injector B, Station 1

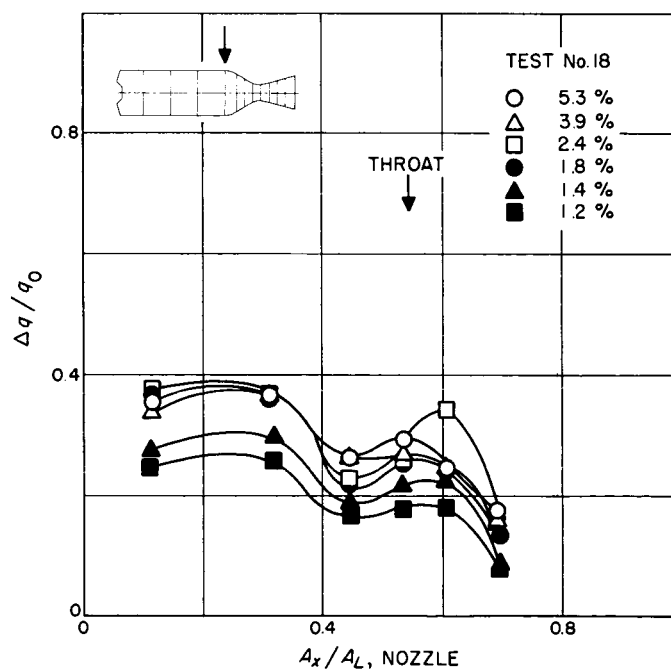


Figure 23. Local reduction in heat flux; 60-octane gasoline, Injector 5, Station 2

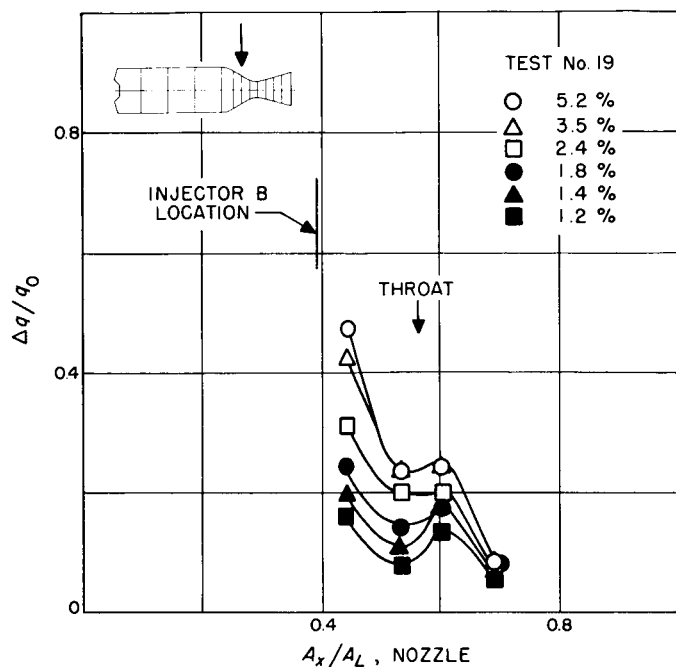


Figure 24. Local reduction in heat flux; 60-octane gasoline, Injector B, Station 1

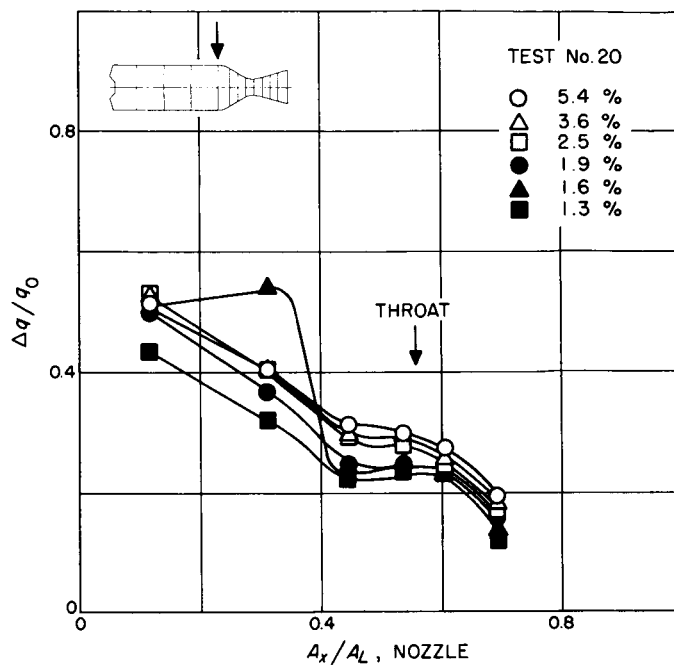


Figure 25. Local reduction in heat flux; methyl alcohol, Injector 5, Station 2

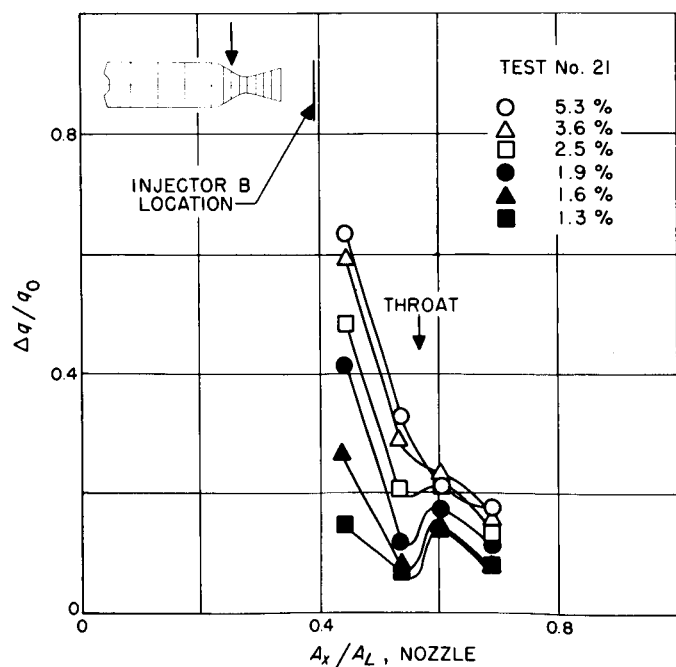


Figure 26. Local reduction in heat flux; methyl alcohol, Injector B, Station 1

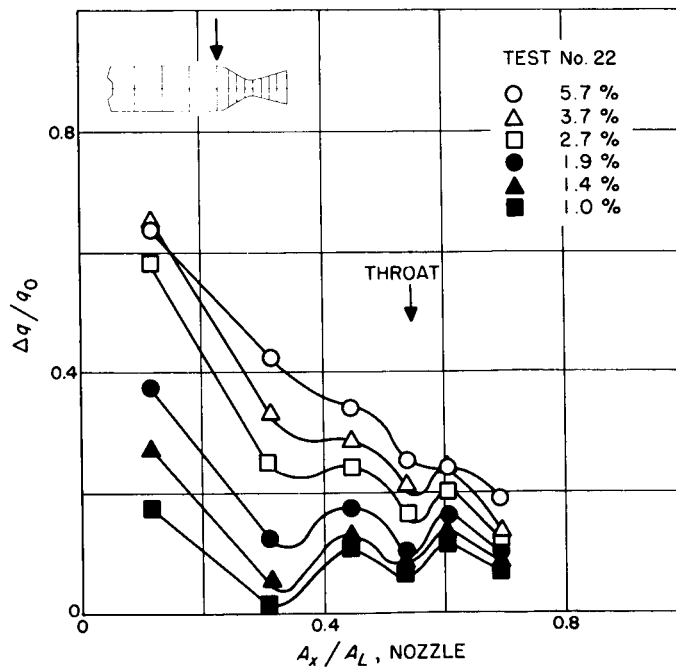


Figure 27. Local reduction in heat flux; ammonia, Injector 5, Station 2

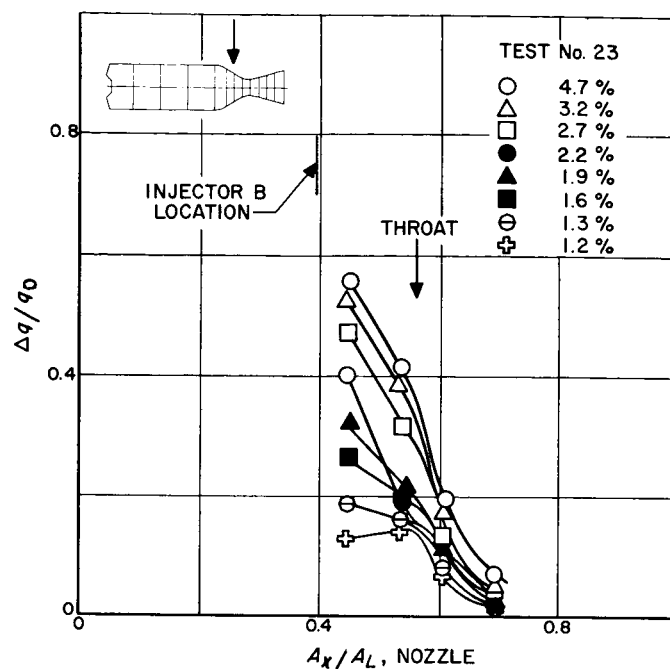


Figure 28. Local reduction in heat flux; ammonia, Injector B, Station 1

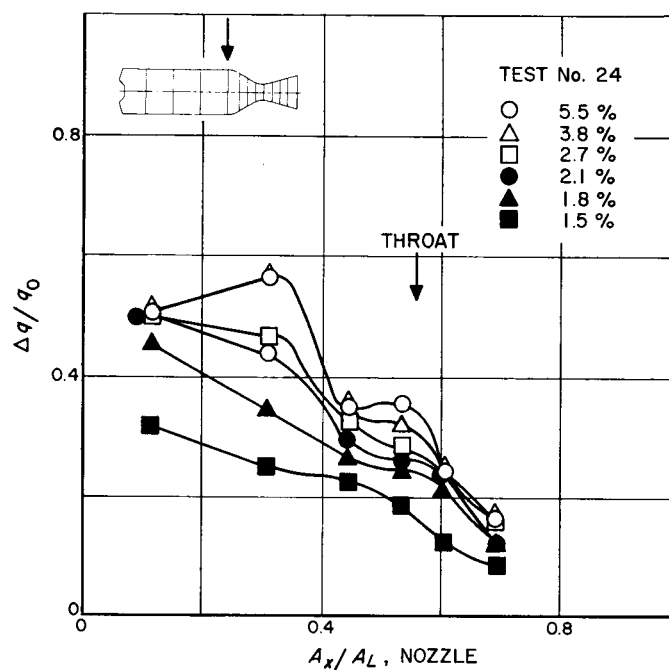


Figure 29. Local reduction in heat flux; jet fuel, Injector 5, Station 2

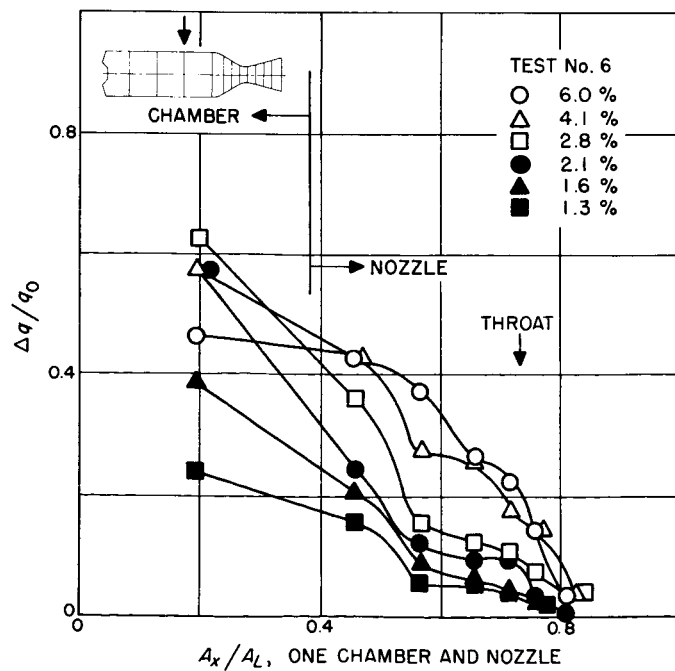


Figure 30. Local reduction in heat flux; water, Injector 5, Station 3

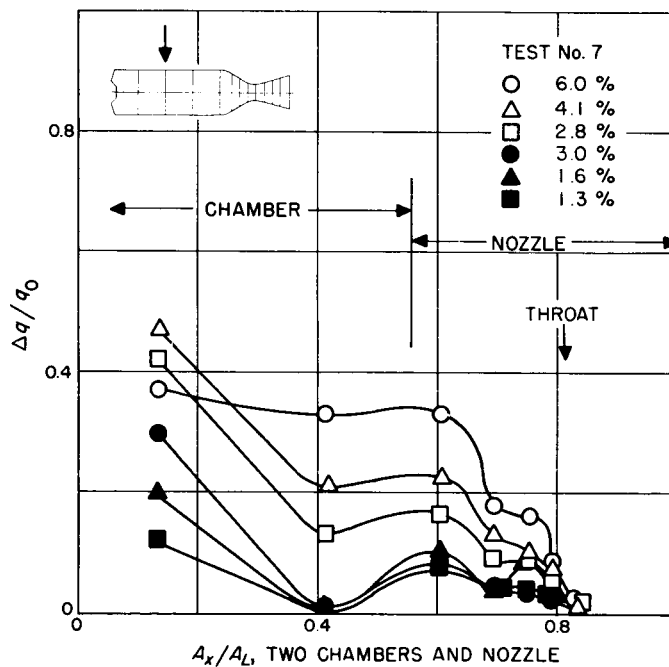


Figure 31. Local reduction in heat flux; water, Injector 5, Station 4

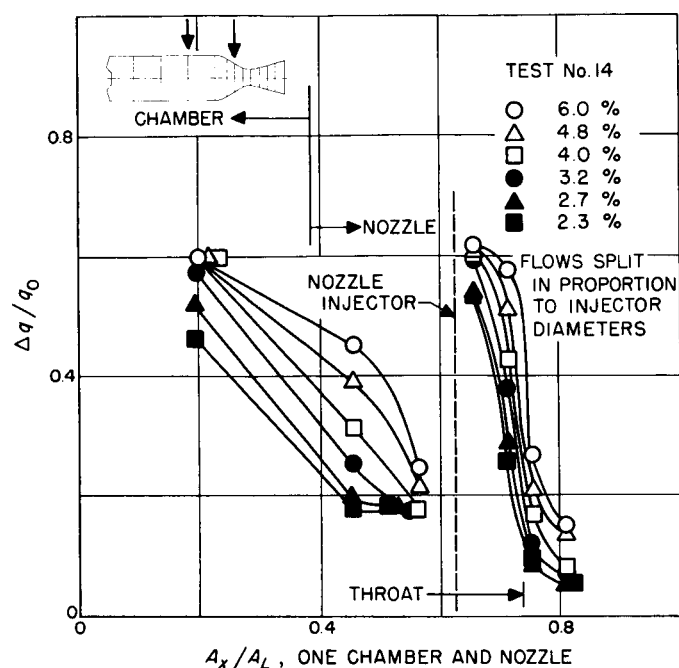


Figure 32. Local reduction in heat flux; water, Injectors B and 5, Stations 1 and 3

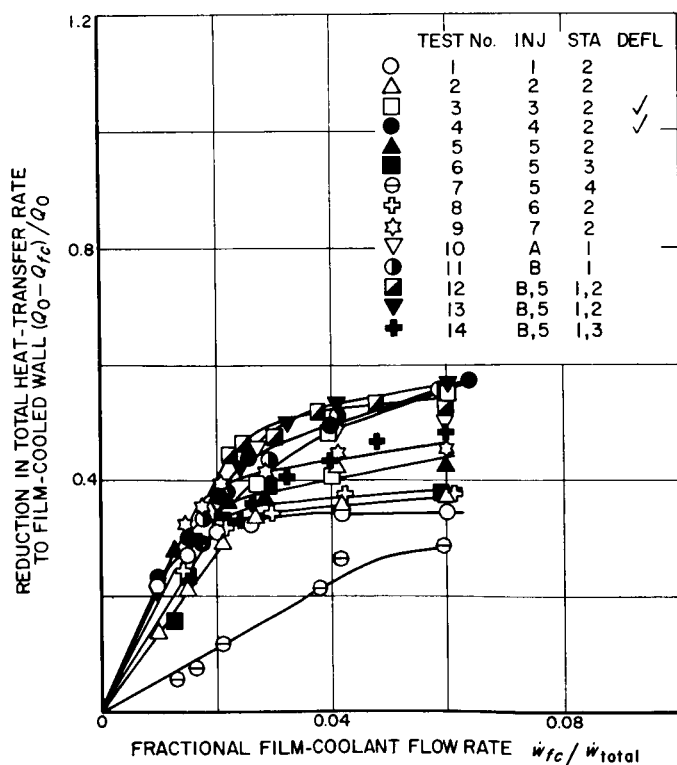


Figure 33. Comparison of performance of all injectors with water used as film coolant

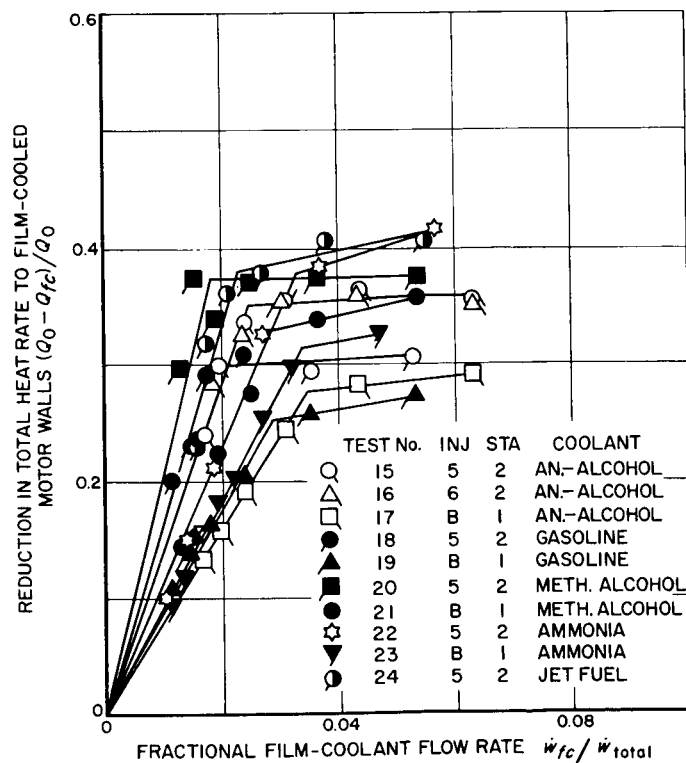


Figure 34. Comparison of organic film-coolant performance

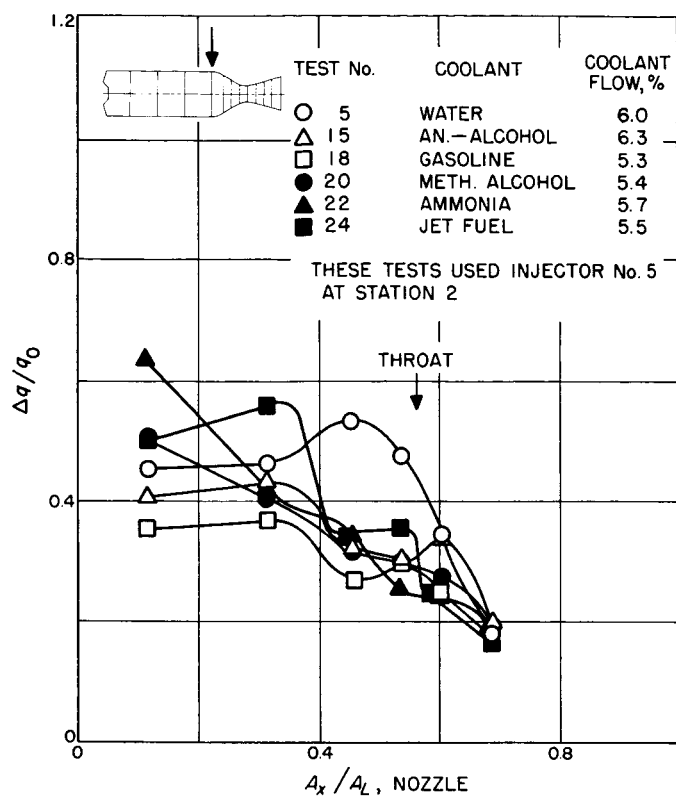


Figure 35. Comparison of local cooling performance of all coolant types

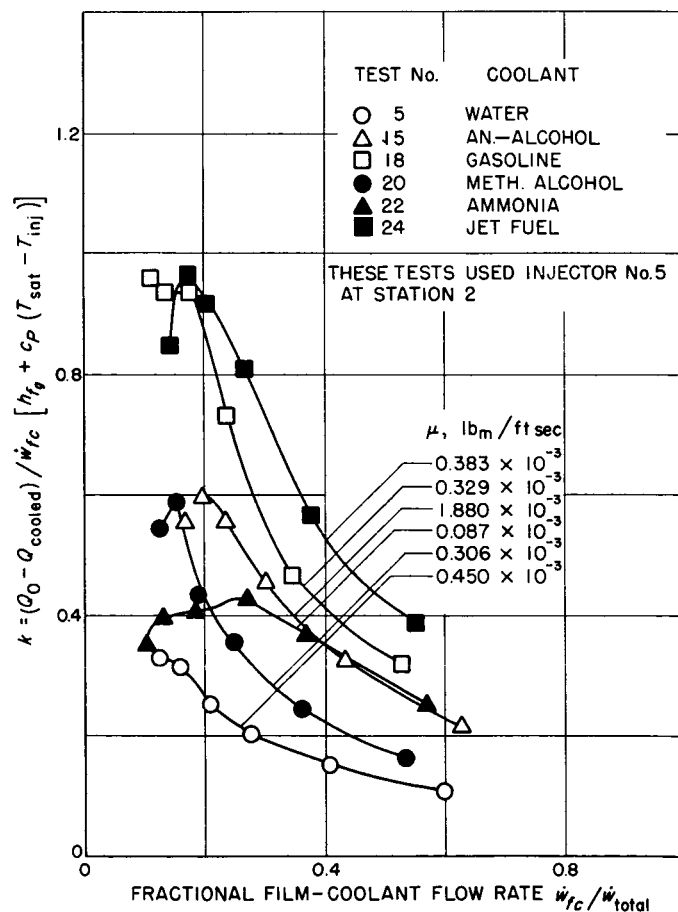


Figure 36. Cooling effectiveness K for all coolants, where $K = (Q_0 - Q_{\text{cooled}}) / \{\dot{w}_{fc} [h_{fg} + c_p(T_{\text{sat}} - T_{\text{inj}})]\}$

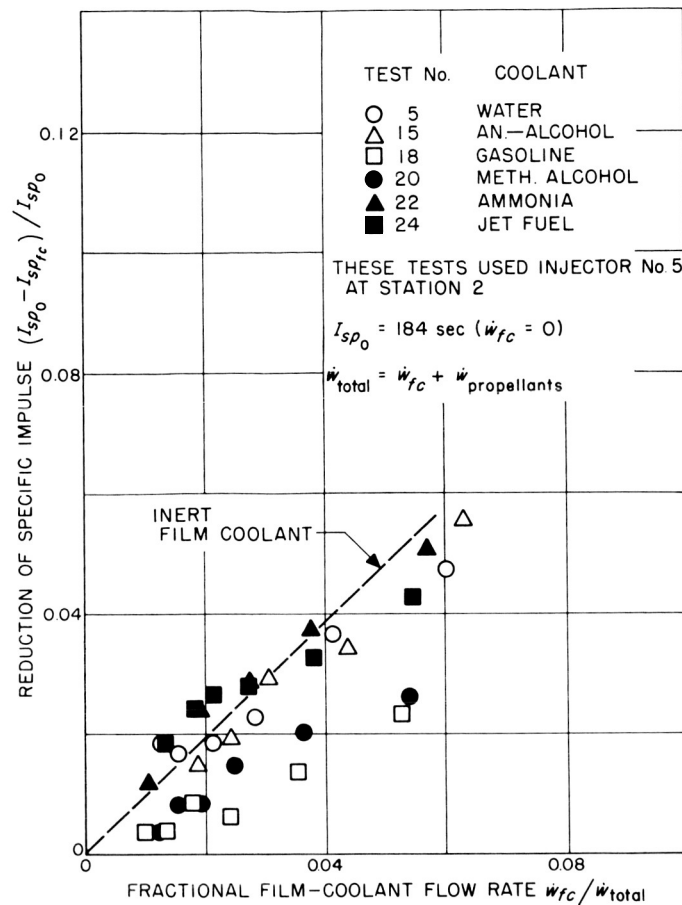


Figure 37. Motor-performance decrease with film cooling

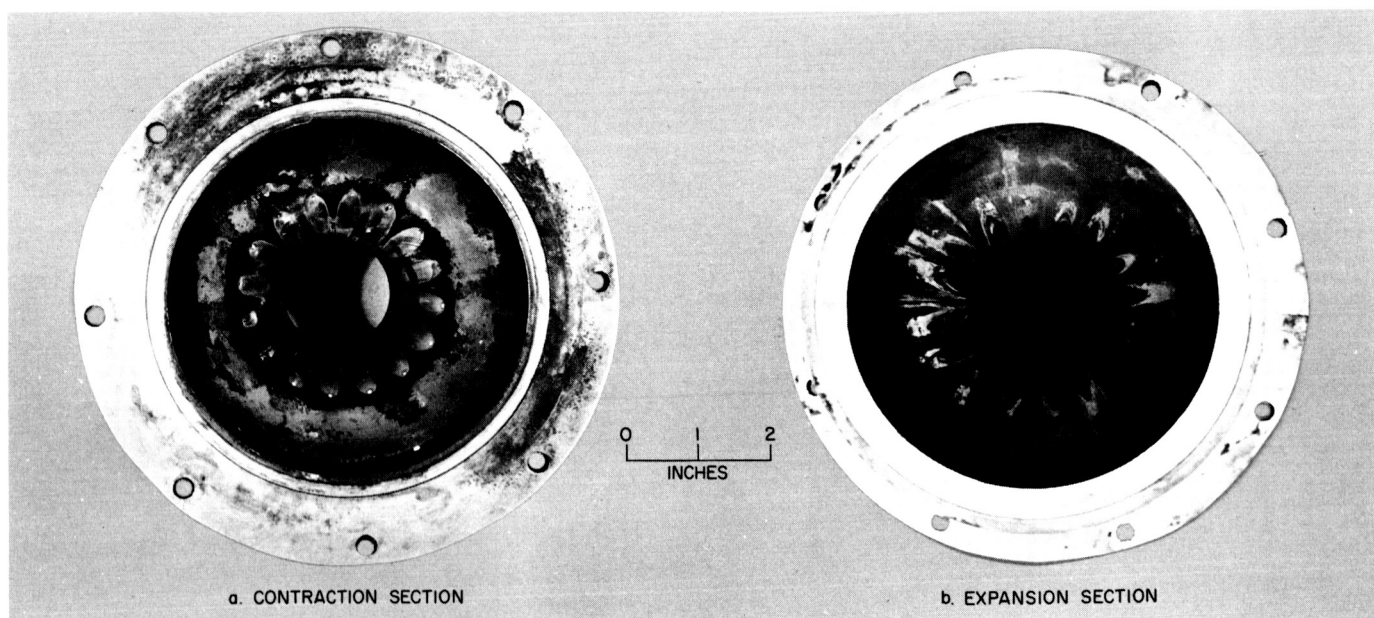


Figure 38. Film patterns on nozzle surface

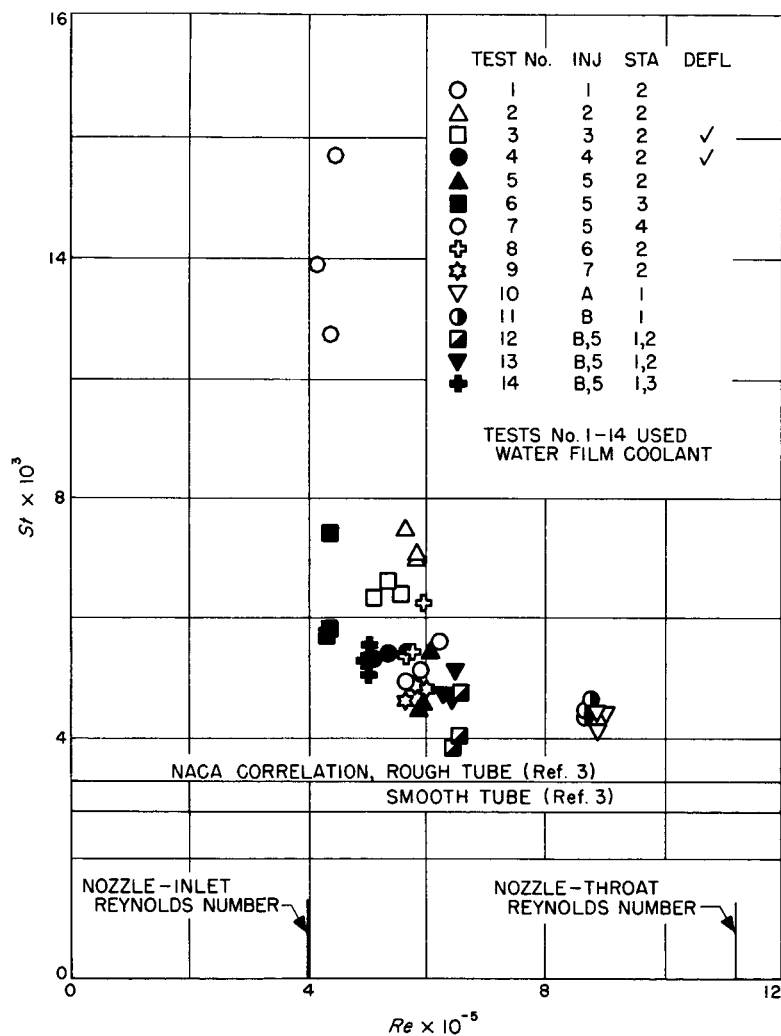


Figure 39. Stanton number comparison with NACA results